UNITED STATES DEPARTMENT OF THE INTERIOR

GEOLOGICAL SURVEY

Reprocessing of USGS Multichannel Line 6

(off Cape May, New Jersey)

by

B. Ann Swift[1], Myung W. Lee[2], and Warren F. Agena[2]

U.S. Geological Survey

Open File Report 88-551

[1]U.S. Geological Survey, Woods Hole, MA 02543
[2]U.S. Geological Survey, Box 25046, Denver Federal Center, Denver, CO 80225

1988

TABLE OF CONTENTS

ILLUSTRATIONS

TABLES

INTRODUCTION

Multichannel seismic reflection lines were collected by the U.S. Geological Survey (USGS) in the early-to mid-1970's as part of a reconnaissance grid covering Baltimore Canyon trough and other basins on the U.S. Atlantic continental margin. The original processed sections, used originally for a basin-wide description of seismic stratigraphy and tectonic framework, fail to adequately resolve details of the buried Jurassic-Cretaceous paleoshelf reef complex (area shown in hachured lines in Figure 1). Reprocessing of the older lines was begun to determine if signal enhancement and processing techniques developed in the last 13 years could improve the imaging of the paleoshelf complex.

Reprocessing goals were (1) to increase coherency and continuity of reflectors, looking closely at resolution and polarity of seismic events; (2) to increase vertical resolution of seismic events in and near the reef complex; and (3) to process the data 48-fold and determine the difference between this and the original 36-fold processing.

A portion of Line 6, a 444-km line off Cape May, New Jersey, was selected for two reasons (Figure 1). First, as one of the oldest lines in the basin, reprocessing might offer the greatest improvement; and second, its proximity to commercial wells makes the data useful for age and stratigraphic correlation, and any improvement in quality would reflect upon the accuracy of that correlation.

DATA ACQUISITION

Line 6 was contractually acquired in 1974 aboard the M/V Gulf Seal by Digicon Geophysical Corporation using a DFS III system and a 1700 in^3 airgun array as the source. Airguns, towed at 9.1 m depth, were fired every 50 m. For this line, there are two firings of the airguns, or pops, for each 'shot point'. Shot point in the original record is a navigational reference point. The 48-channel cable was a total of 3600 m in length, with a non-linear configuration: 50 m spacing for the far 24 groups (channels 1-24); 100 m spacing for the near 24 groups (channels 25-48); and a 75 m space at the transition between channels 24 and 25 (Figure 2A). This configuration was used to optimize resolution of normal moveout in the far traces. The streamer was towed at a depth ranging from 14 to 18 m. The inline shot offset was 348 m, from the center of the gun array to the center of the near channel. The data were recorded in SEGA format, at a sample rate of 4 ms, with anti-aliasing filters set at 8 to 62 Hz. Record length was 11 s over the shelf and increased first to 12 s, then to 13 s over the slope and in deep water.

Line 6 has 4443 shot points (SP 210-4652, which corresponds to 8886 'pops') and extends out into deep water over oceanic crust. Of these, only SP 210 thru 3200 were included in the original processing due to funding constraints. The remainder of the line which has never been processed is currently being processed (Swift, unpublished data).

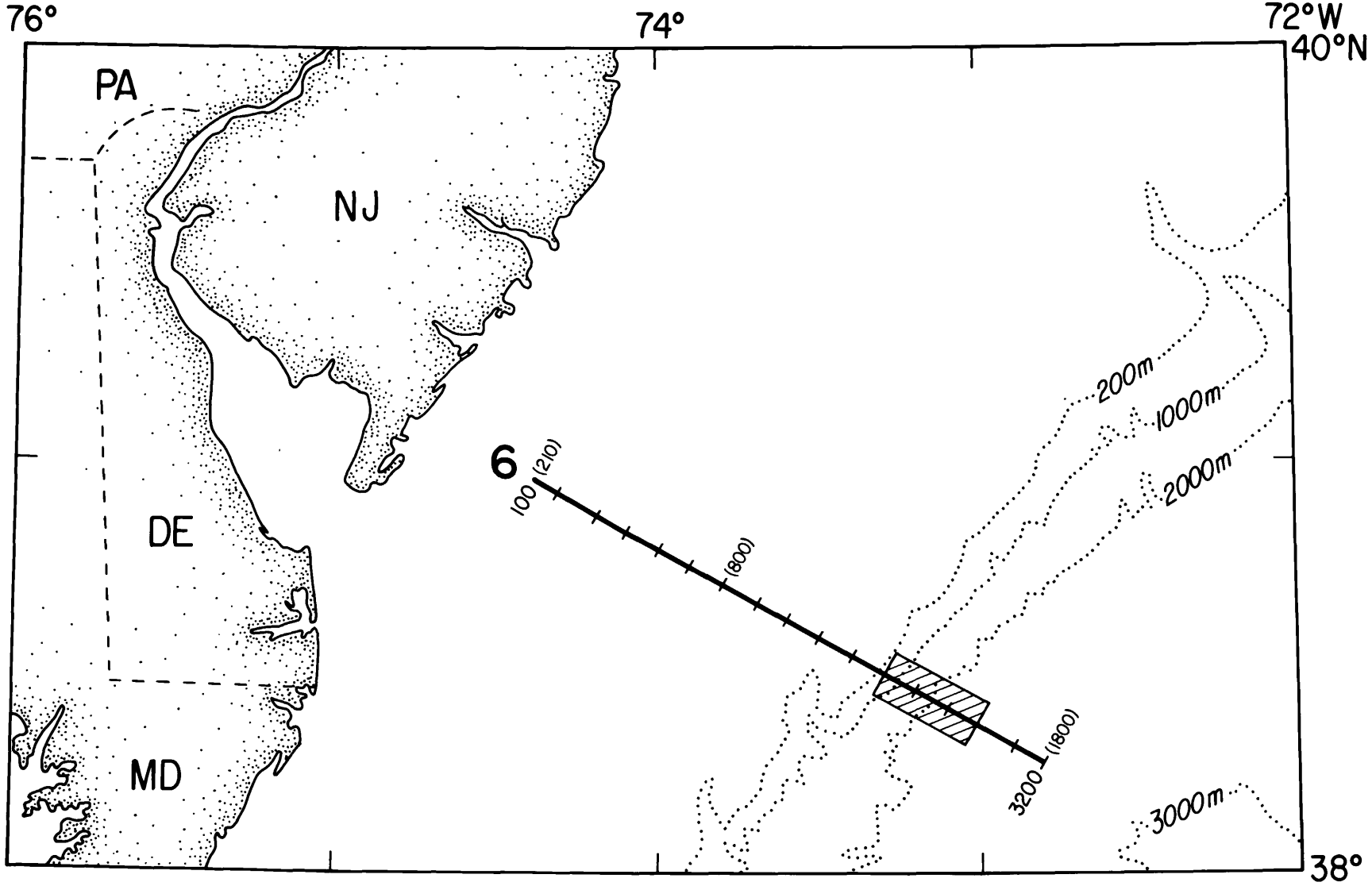

FIGURE 1: Location map for Line 6. Bathymetry is shown in meters. Tics are every 100 shot points (=200 pops), with original shot numbers in parentheses. Approximate area of Jurassic reef complex is hachured.

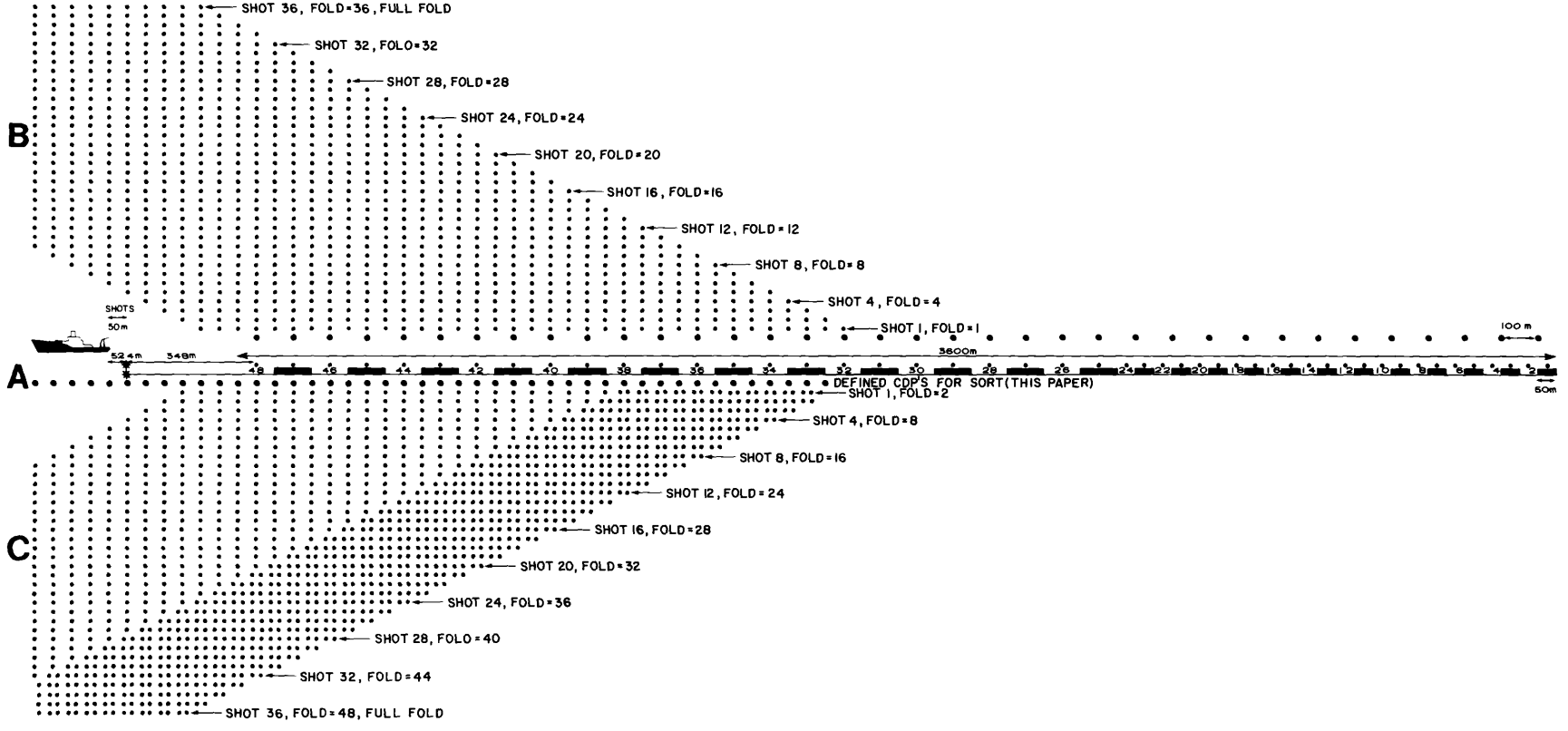

FIGURE 2: Cable configuration and line geometries.
A: Cable towed by Gulf Seal.
B: Geometry resulting from GSI 2-to-1 compression of far 24 traces. Large dots show group centers used in processing. Smaller dots show development of fold with succesive shots.
C: Geometry used in reprocessing.

ORIGINAL PROCESSING

The line was originally processed (Table 1) by Geophysical Service Inc. (GSI) as 36-fold data, which was accomplished by a 2-to-1 compression with a differential normal moveout correction of the far 24 channels. The adjusted line geometry was then linear, the equivalent of 36 geophones spaced at 100 m intervals (Figure 2B).

A spherical divergence correction was applied to the demultiplexed traces to correct for geometrical spreading and therefore, attenuation of the seismic-source wave amplitude with distance from the airgun array. Two nonnormalized time-variant deconvolution filters were applied. Specific design and application parameters were not provided by GSI. Lengths and design gates were offset- and water-depth dependent.

Stacking velocities were determined from velocity analyses every 60 shots (about 3 km) at seven depths for each location. Normal moveout corrections were applied along the line using interpreted stacking velocity functions at the analysis locations and interpolated values in between. The stack was 36-fold and had an inverse square root of fold-amplitude scaling recovery to compensate for the fold difference due to the mute applied.

Post-stack processing was application of a nonnormalized digital time variant bandpass filter: 10-35 Hz for the 0 to 1.65 s range and 5-25 Hz for the 4 to 9 s range with interpolated values between the two specified ranges.

REPROCESSING

The section of Line 6 chosen for reprocessing covers the landward end, the mid-basin, the present shelf edge, slope and upper rise, and oceanic crust. It is the original SP 210 thru 1800, or 3180 shots ('pops') that have been reprocessed.

The data were demultiplexed with early gain removal and sorted to yield 48-fold coverage. This was accomplished by defining the geometry such that the common depth points (CDP's) are evenly spaced every 50 m, but are located unequal distances from the channels which lie to either side (Figure 2C). The traces are then essentially smeared in the CDP domain (gathered to a defined CDP which lies between the two true CDP's, see Figure 2C) which allows for greater fold coverage. This contrasts with the 2:1 compression applied in the original processing, which results in smearing in the shot domain and reduces fold.

In the landward 1400 shot points, the shot gathers showed a transient yet coherent, negatively dipping noise (examples for shot points 301 and 451 are shown in Figure 3A) which the GSI-processed stacked section indicates originates in shallow side-scatterers. The noise was lessened in the GSI-processed section by low pass filtering to 25 Hz. In the reprocessing however, we wanted to preserve the higher (signal) frequencies to sharpen reflectors.

The noise has a marked moveout difference from the signal in the shot domain when compared to the CDP domain, where a similarity in moveout causes the noise to stack coherently (Larner et al., 1983). The method we selected for suppresion of this coherent noise is a two-dimensional frequency vs wavenumber (F-K) dip filter which removes or passes coherent energy in a specified range in the shot

TABLE 1: LINE 6 ORIGINAL PROCESSING

DEMULTIPLEX
|
2-1-COMPRESSION OF FAR 24 TRACES
|
SORT -- 36 FOLD
|
SPHERICAL DIVERGENCE CORRECTION
|
DECONVOLUTION
|
NORMAL MOVEOUT CORRECTION
|
STACK
|
BANDPASS FILTER
|
MIGRATION

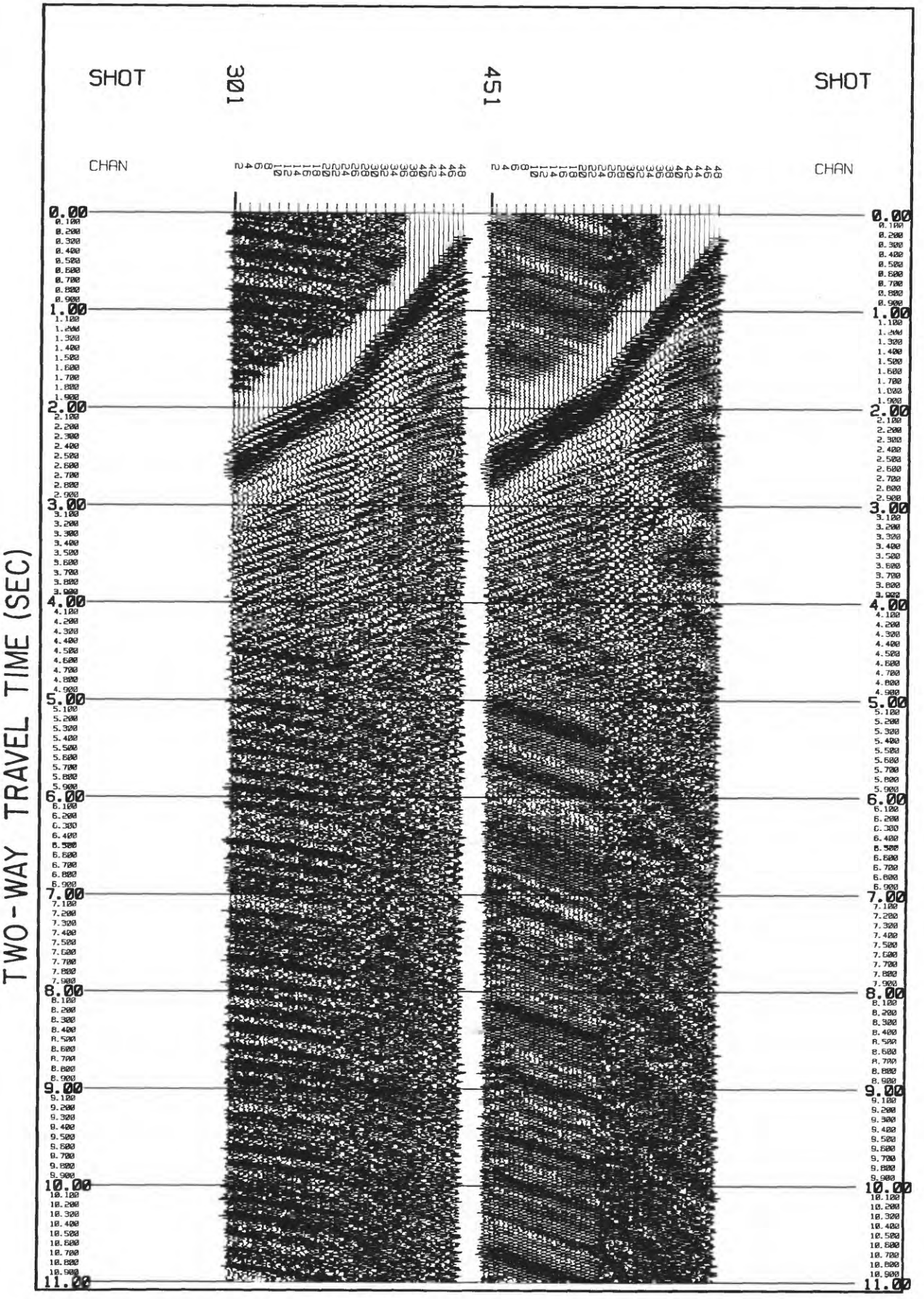

FIGURE 3: Shot gathers with spherical divergence correction, AGC 500, bandpass filter (8/12 to 50/62 Hz) and gain applied for display purposes.
A: Gathers exhibiting negatively dipping noise in the landward portion.

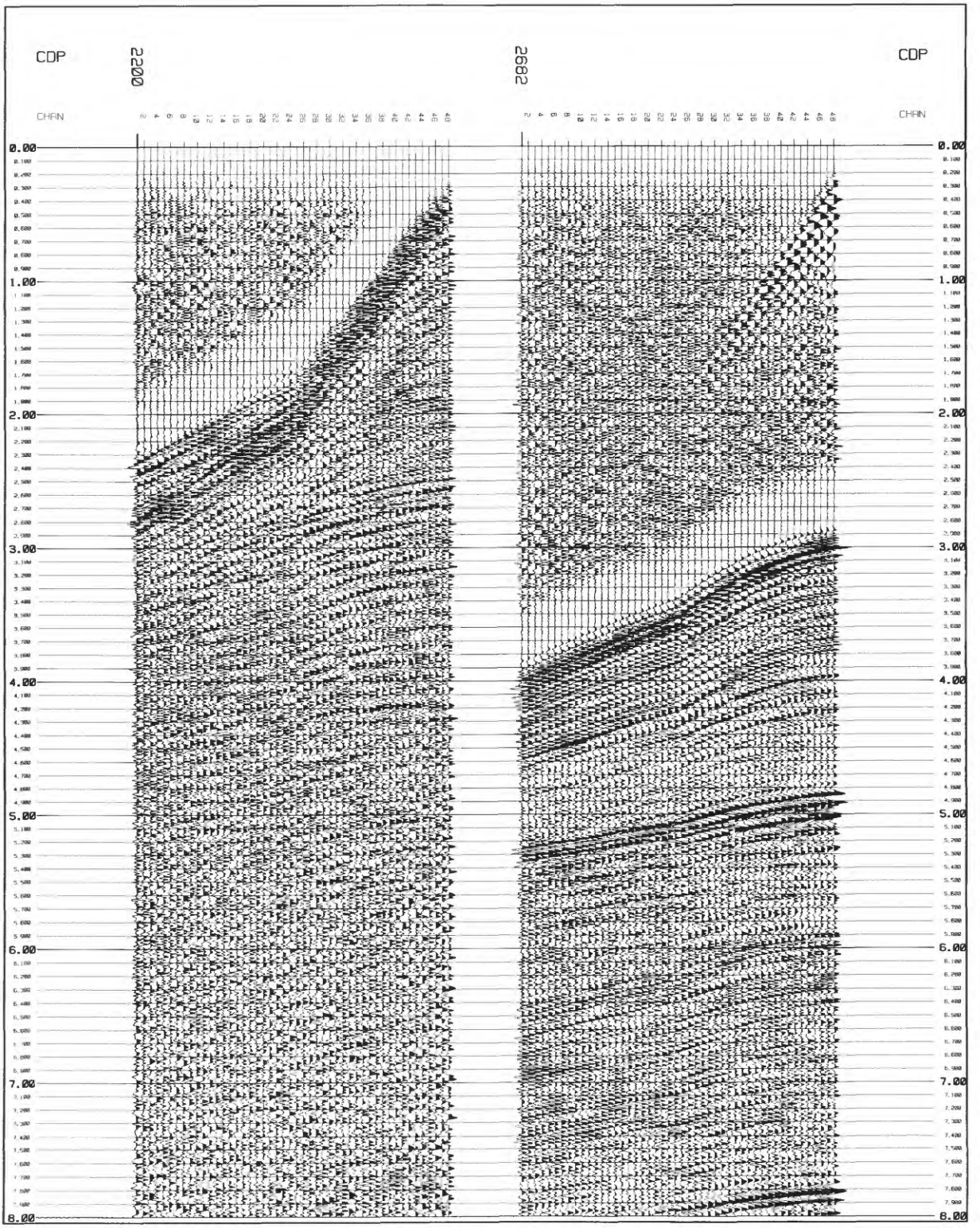

FIGURE 3B: Gathers farther seaward -- no dominant coherent noise patterns.

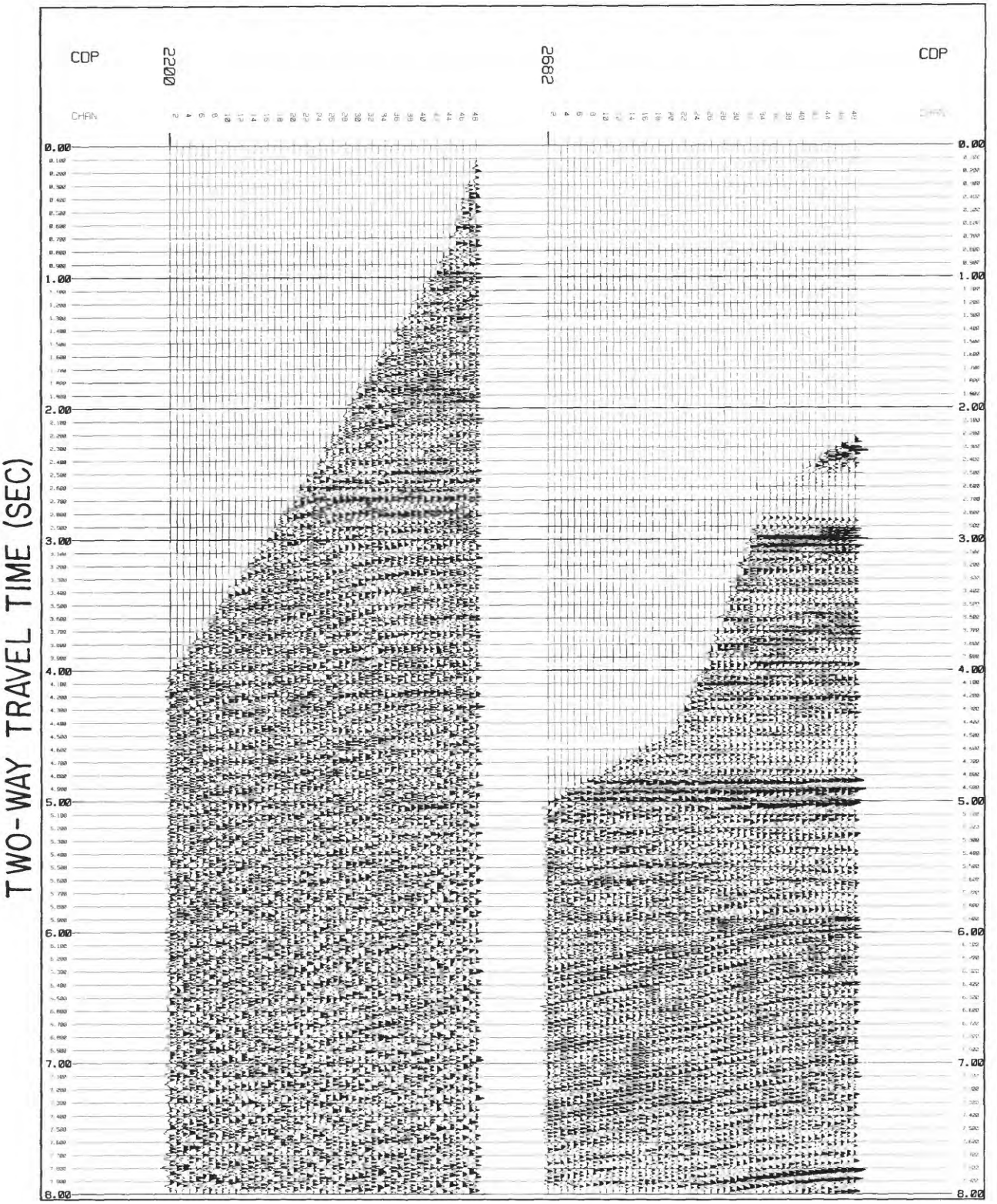

FIGURE 3C: Gathers after mute and normal moveout correction.

domain (Larner et al., 1983). The dip filtering is best applied in the shot domain where there is a significant moveout difference between signal and coherent noise. Dip filtering is a time-intensive step in the processing and is needed only where the coherent noise is present. Therefore, we split the line in two sections for processing; the landward section, which required the F-K filter, and the seaward section, which was not contaminated with coherent noise (Figure 3B).

LANDWARD SECTION

Processing of the landward portion of the line was complicated by the presence of a coherent noise pattern evident in the shot domain. We did spectral analysis of the traces in the noisy shot gathers to check if notch or bandstop filtering would remove the noise while preserving the higher signal frequencies. The spectral analysis showed a noise frequency-content variability not only between shots but also between channels within a single shot. The near traces tend to be richer in the lower frequencies and the far traces, in the higher frequencies. Therefore, notch or bandstop filtering was ruled out as a viable method of noise suppression on these data and we proceeded with the F-K filtering.

In order to determine the proper F-K (dip) filter to apply, a two-dimensional F-K analysis was performed (Figure 4A). This process was complicated by the nonlinear cable configuration which causes an apparent change in dip of the reflectors between the near and far 24 channels and by possible differences in the array response between the inner and outer 24 channels. The near 24 channels were contaminated more by the water-bottom multiples and the far 24 channels were contaminated more by side scattered energy (Figure 3A). To resolve this, the F-K analysis was performed on the far 24 channels between 4 and 10 s in order to select parameters for dip filtering (Figure 4A).

The dominant coherent noise is characterized by a broad frequency band (15-55 Hz) and negative-dipping linear moveout that has an apparent velocity of approximately 3100 m/s (right half of the F-K plot, Figure 4A). This coherent noise is aliased above 30 Hz and appears as a linear event on the left half of the F-K plot (Figure 4A). The coherent noise is dominant in the plot, so it is difficult to identify any coherent signal. The signal is apparent as a positive-dipping event on the left half of the F-K plot and the possible signal band, about 24 Db below the noise level as indicated in Figure 4A. We assumed that all negative-dipping events and positive-dipping events whose apparent velocities were less than 6250 m/s below 3 s are noise, judging by the GSI-processed section and analysis of other shot gathers. Thus dips within the -8 to 0 ms/trace were passed in the shot domain. The dip-filter length was 248 ms (31 x number of trace sample points); its width was 13 traces, applied to all traces within the shot below 3 s. A frequency filter of 4 to 40 Hz was selected. The 40 Hz high cut was applied in order to avoid possible aliasing of the coherent noises. The dip filter was applied to the traces in the 3 to 11 s range because of the lack of a dominant noise pattern in the section above and to circumvent the nonlinearity problem in the uppermost section (0-3 s) that is evidenced as abrupt changes in moveout of both signal and noise between channels 24 and 25.

After processing with the dip filter, the unfiltered upper 2.5 s of data was merged with the lower dip-filtered 3-11 s, using an overlapping window beween

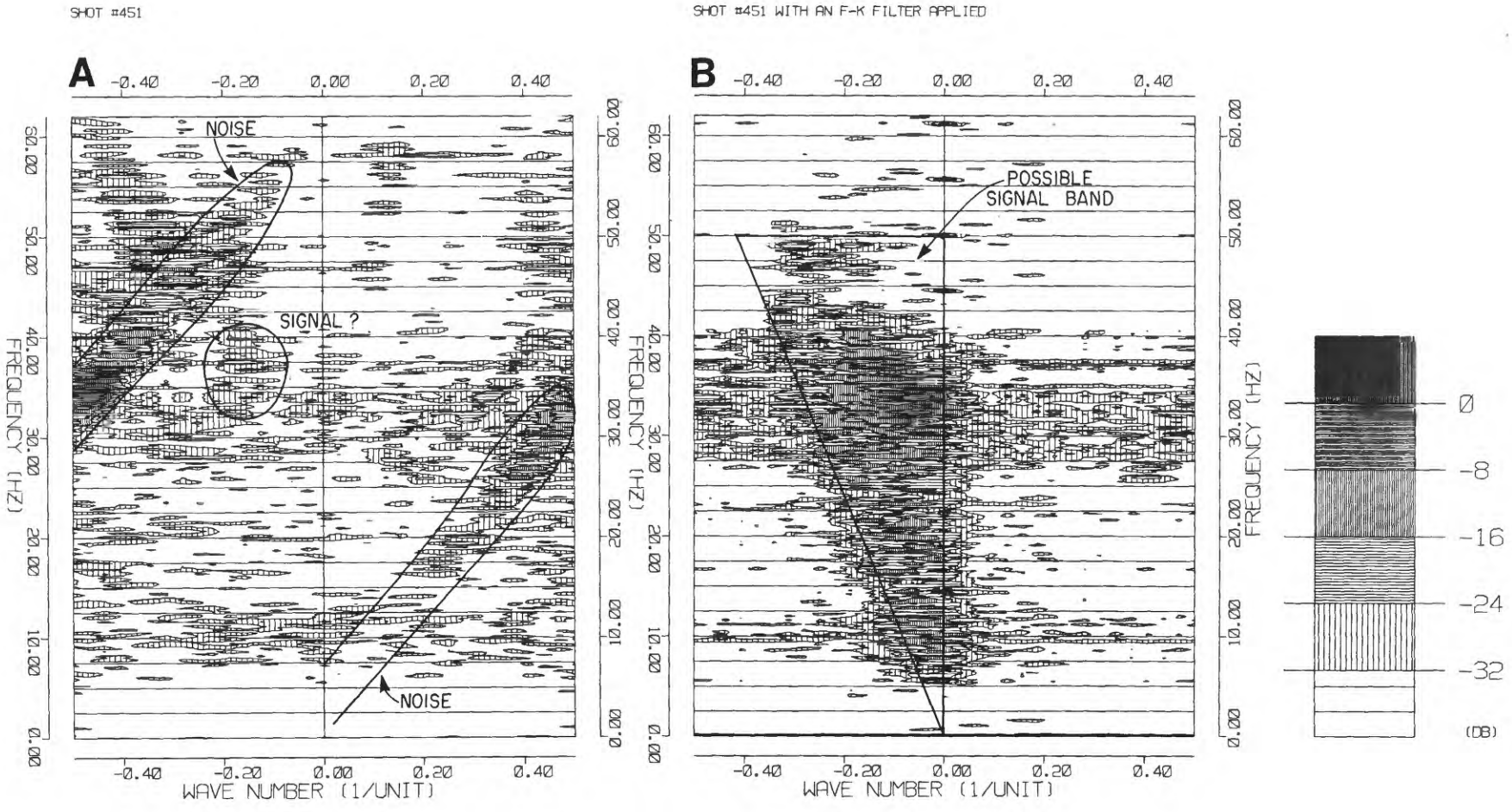

FIGURE 4: F-K analysis of shot 451, in the time range of 4-10s. Plots are amplitude contours of wave number vs. frequency (Hz). There are five contour levels, shown by lines of varying density, each representing a 10 decibel range. Slope of dipping events = (wavenumber*trace interval/frequency).
A: Channels 1 through 24, raw data used to design dip filter. Signal (?) and noise are identified.
B: Channels 1 through 24, data after dip filtering, with possible signal band marked.

2.5 and 3 s (technique described by Lee and others, 1988). The dip filtering enhanced positive-dipping events, possibly signals, below 3 s (Figures 4B, 5). The effectiveness of shot-domain dip filtering can be examined on the comparison of stacked sections noting the increased continuity and definition of reflectors in the reprocessed section (Figure 6A and B).

The remaining prestack processing followed standard processing procedure for multichannel data. The 48-fold data were sorted, then a variable gain compensation based on a second-power of two-way travel time, as opposed to an empirical curve, was applied for compensation of seismic amplitude loss. An automatic gain control (AGC) function was then applied over a 1000 ms window to balance the data. Next, a spiking deconvolution was applied with an operator length of 61 (= number of filter points) and 0.1% white noise was added. A normal moveout (NMO) correction was made to correct for the differential in arrival times with increasing offset, arising because the signal is not reflected vertically. The NMO was applied using the original GSI velocities, since a comparison of velocity functions showed no significant differences between the two in this section (Figure 7).

This procedure was followed by mute of direct arrivals and refractions, and a scaled stack. During the stack, a balancing option was supplied in which the traces in each CDP are divided by the maximum fold and then summed. The samples within each trace are then multiplied by a scalar equal to the maximum fold (48) divided by the number of traces having actual samples in the summed sample. This compensates for the variation in amplitude of the data due to the lack of signal early in the recording range for far channels.

Post stack processing consisted of an AGC with a 1000 ms window, a bandpass filter 4/6 to 48/60 Hz, and application of a gapped (predictive) deconvolution operator of length 61, and a gap measured by the second zero crossing of the trace autocorrelation with 3% white noise added. The final time section was plotted after two-dimensional smoothing to reduce the background noise and enhance the coherent reflections. The operator is a two-dimensional filter that replaces the original data value by the sum of the original data value and 50 percent of the average of nine adjacent data values (for details, see Lee and others, 1988; Figure 12).

At this point a comparison was run to determine the effects of the increased fold in the section. The GSI processing sequence could not be reproduced exactly due to a lack of detailed information on the original processing parameters, so a test section of 130 shots was selected and processed 36-fold, following the reprocessing sequence. This was accomplished by "unsorting" the traces that had had the shot-domain processing applied (resample to 8 msec, dip filter for the to 3-11 s range, and merged with the unfiltered top 3 s). The far-24 traces were then compressed 2:1 with a NMO correction and sorted 36-fold. Subsequent processing was identical to that for the 48-fold data (Table 2). A comparison of the two test sections shows that the deeper reflectors may be slightly sharper on the 48-fold section, but the section is not greatly enhanced by the extra 12-fold (Figures 6B,C). The extra fold will not have an effect on the upper section because the application of the mute effectively decreases fold (Figure 3C).

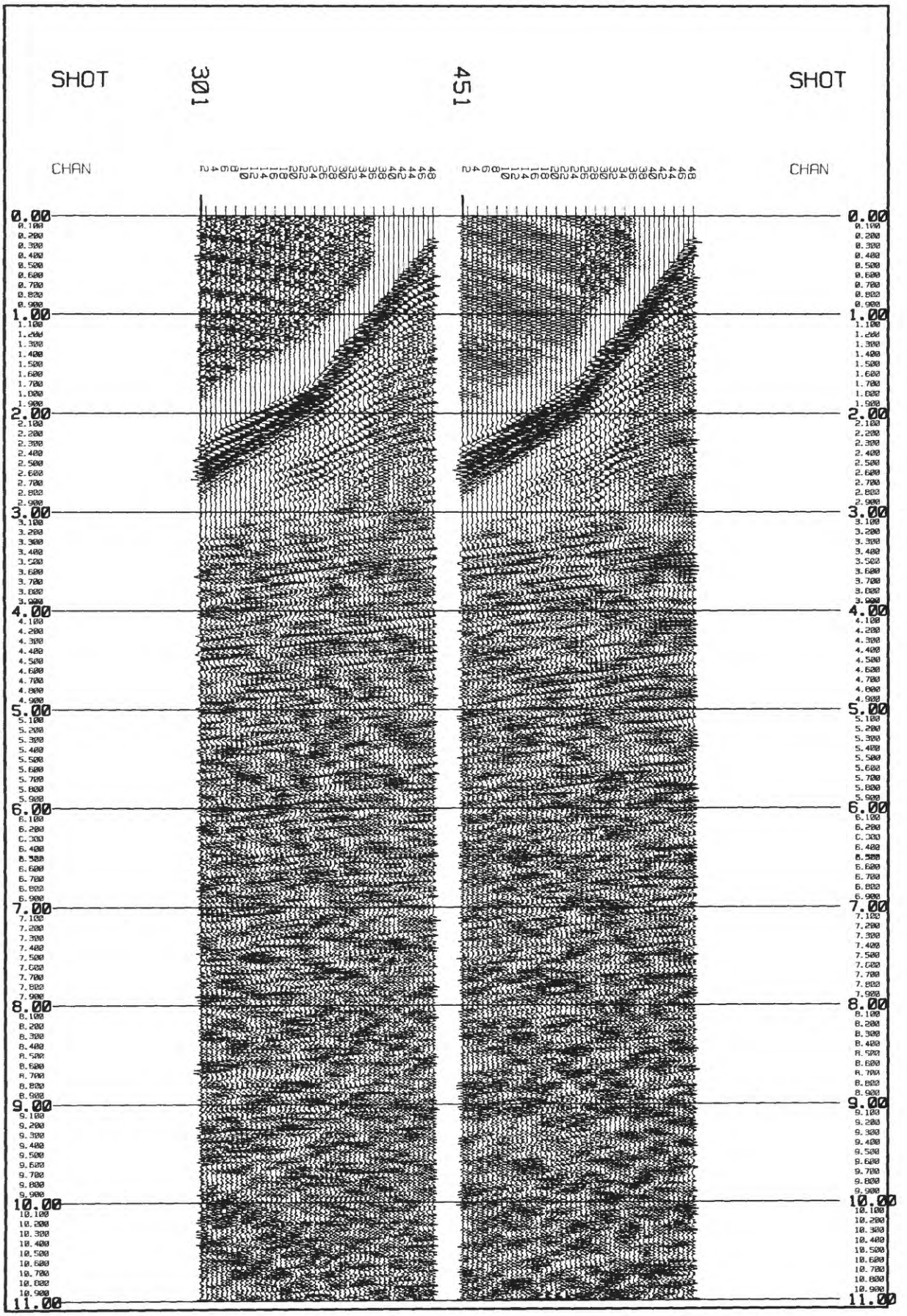

FIGURE 5: Shot gathers after application of dip filter and bandpass filter. Compare to Figure 3A.

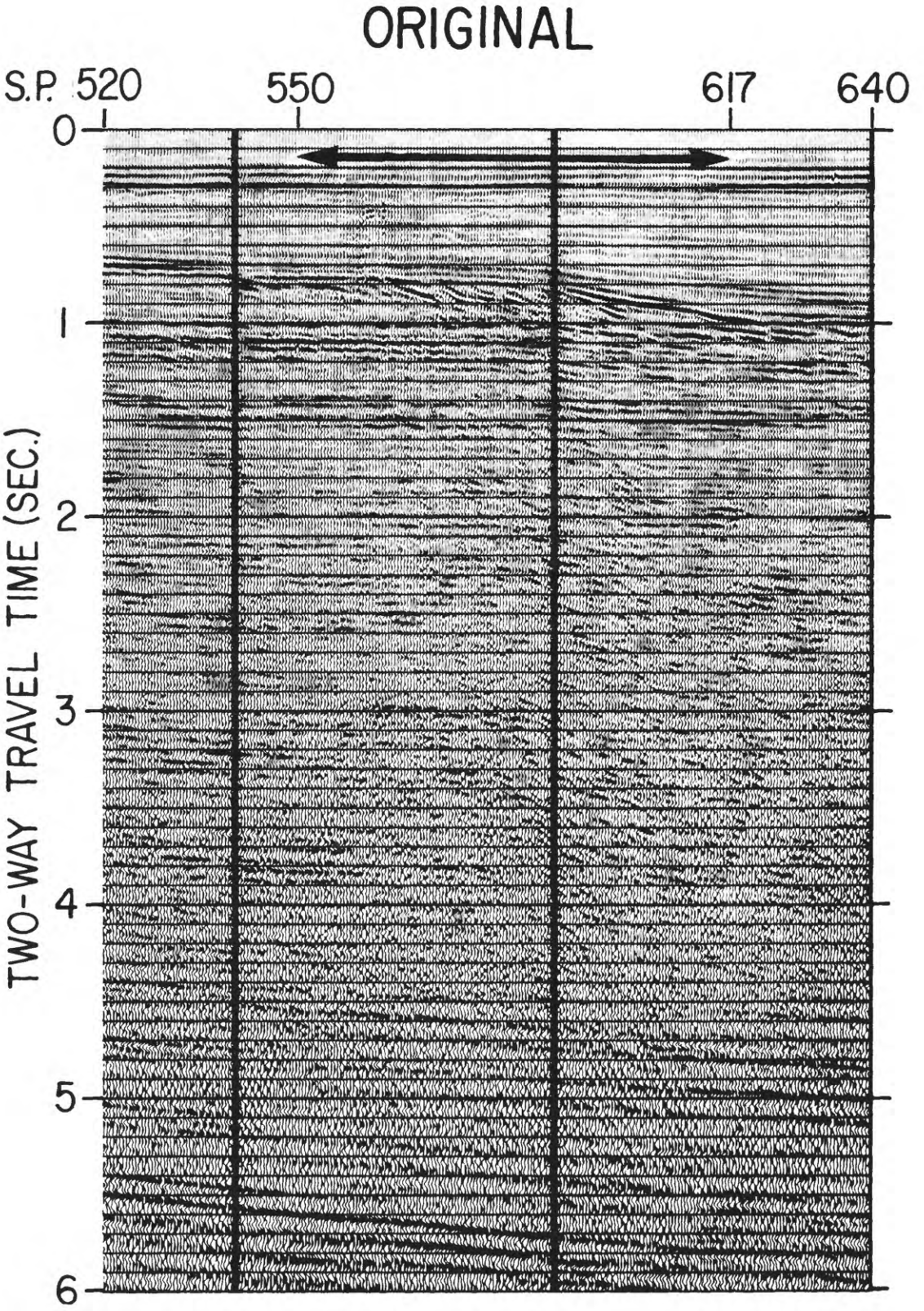

FIGURE 6: Comparison of time section in landward end of line 6.
A: Original GSI processing, shot points 520-640. Section between SP 550 to 617 are shown in B and C.

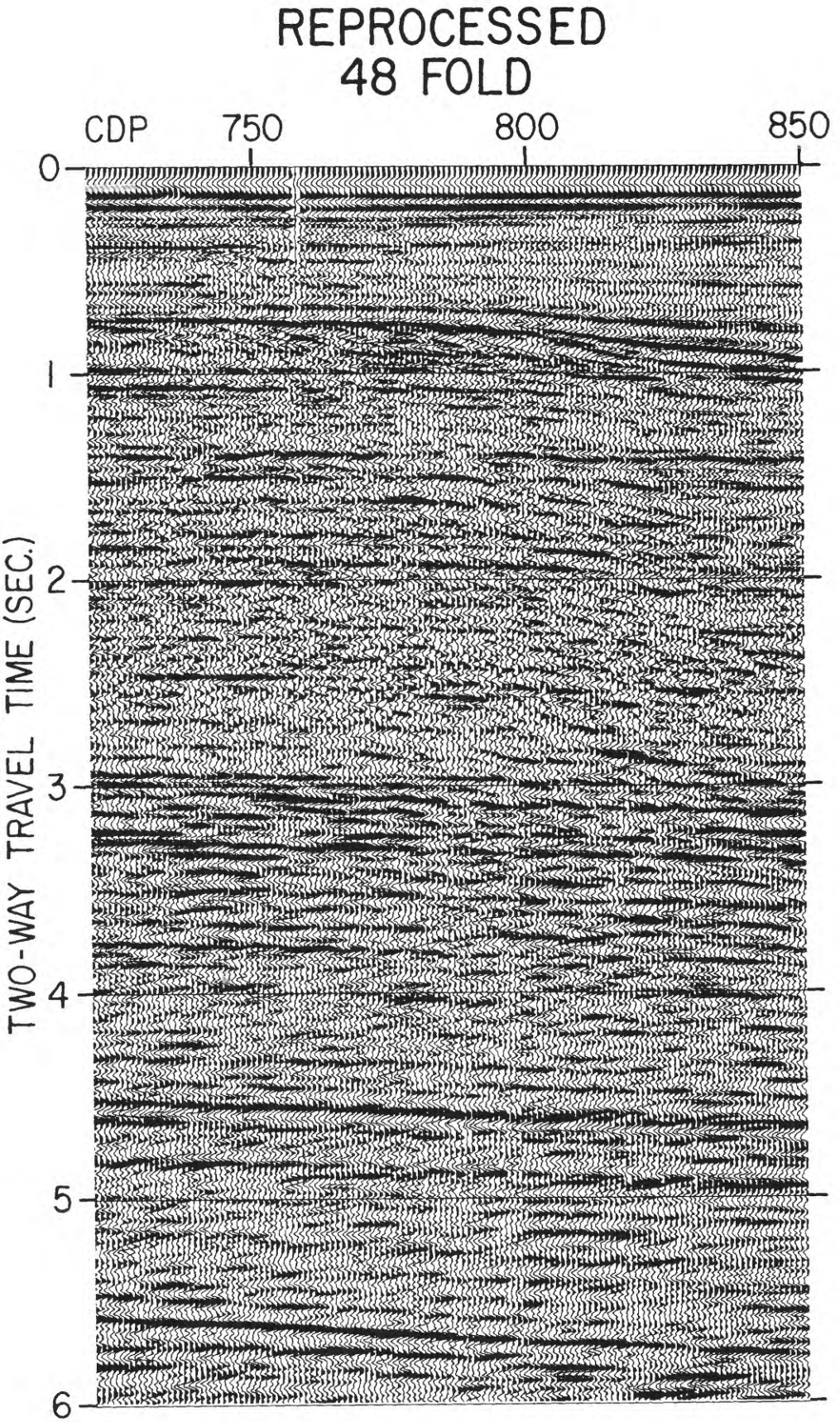

FIGURE 6B: Reprocessed data -- 48 fold.

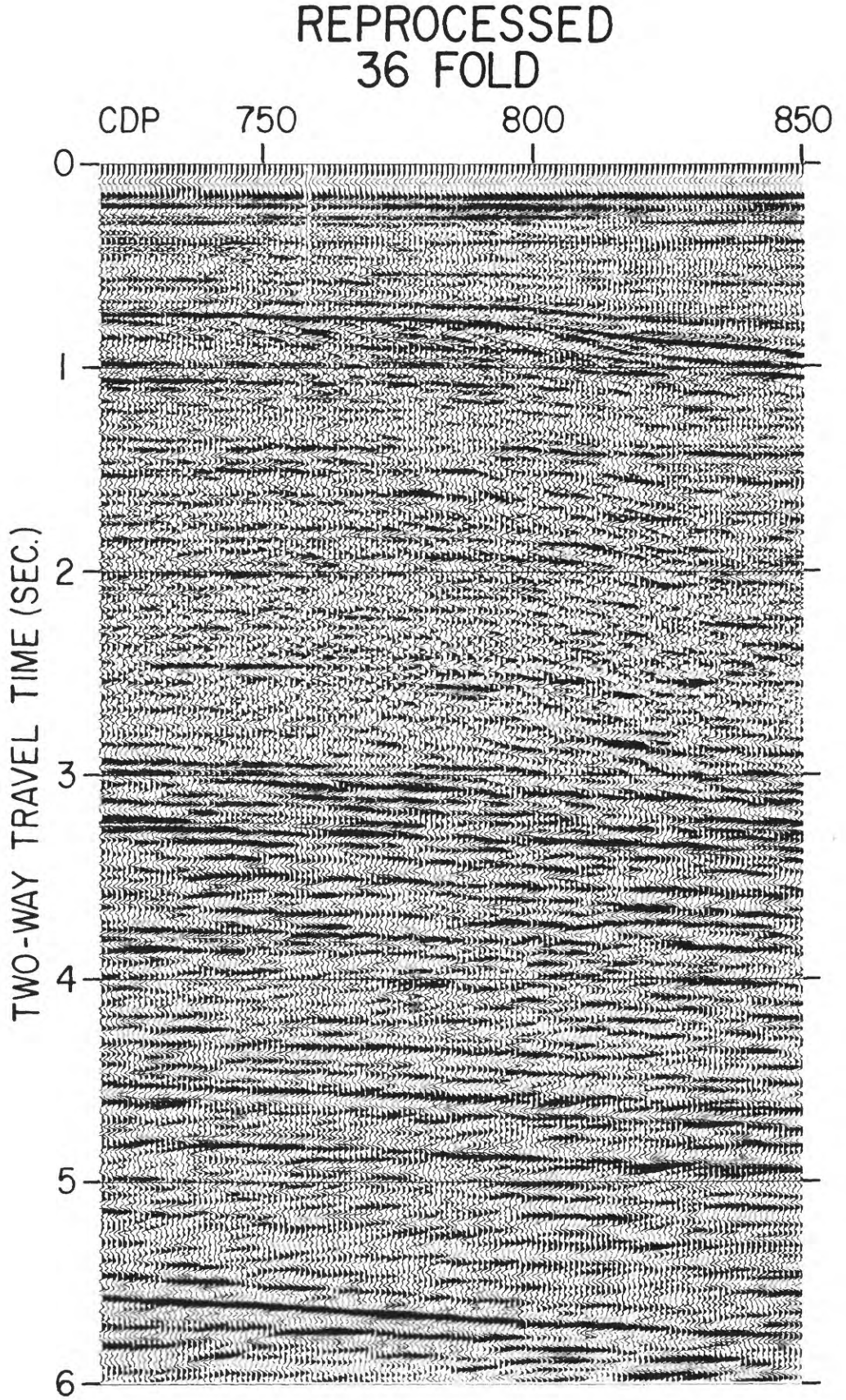

C: Reprocessed data -- 36 fold.

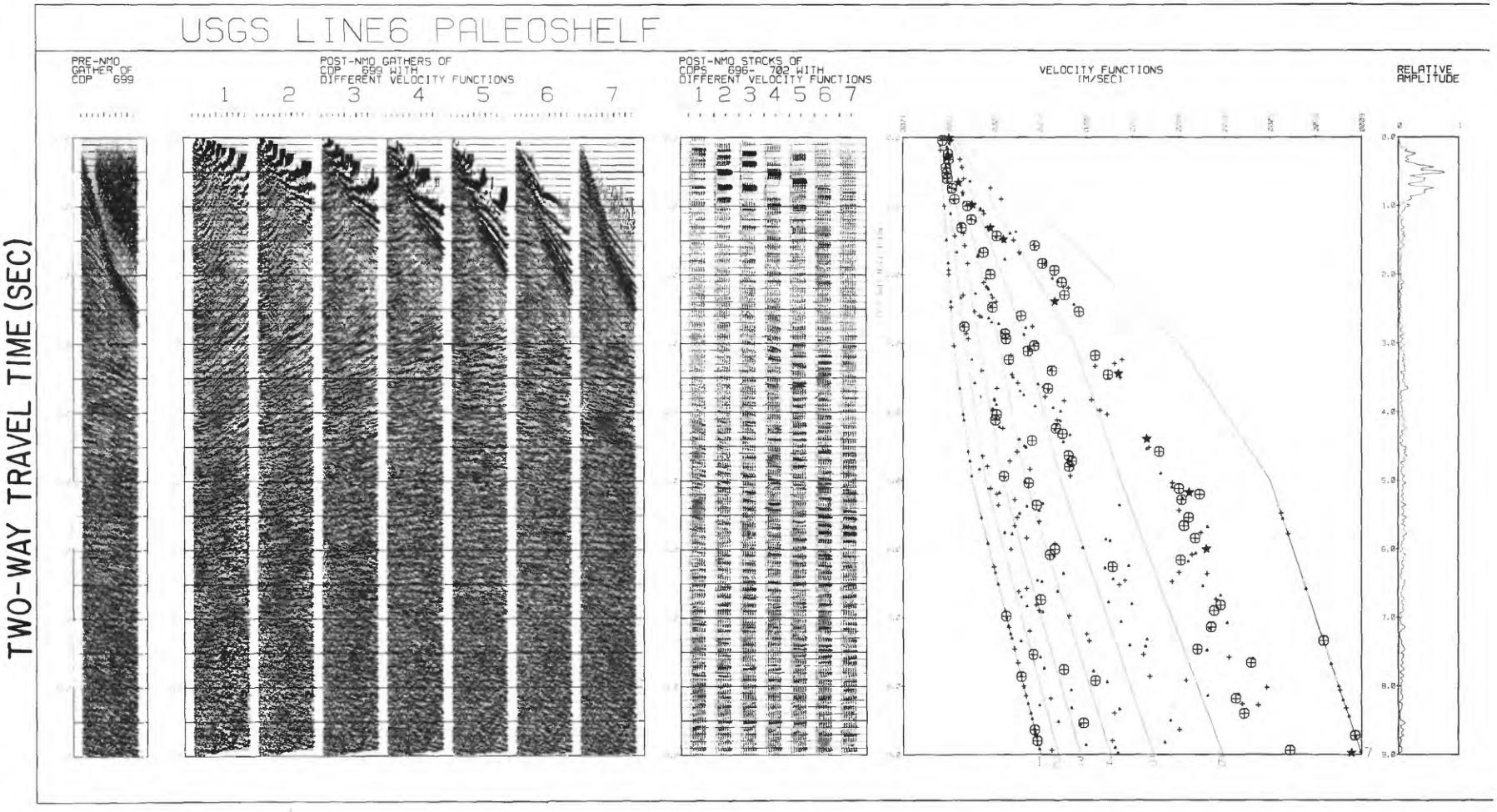

FIGURE 7: Comparison of velocity functions for CDP 699.
Plot shows velocity analysis for reprocessed CDP. Maximum coherence picks are shown by circled crosses, then pluses, with triangles representing picks with the least coherence. Velocity picks used in original processing are shown by stars.

TABLE 2: LINE 6 REPROCESSING SEQUENCES

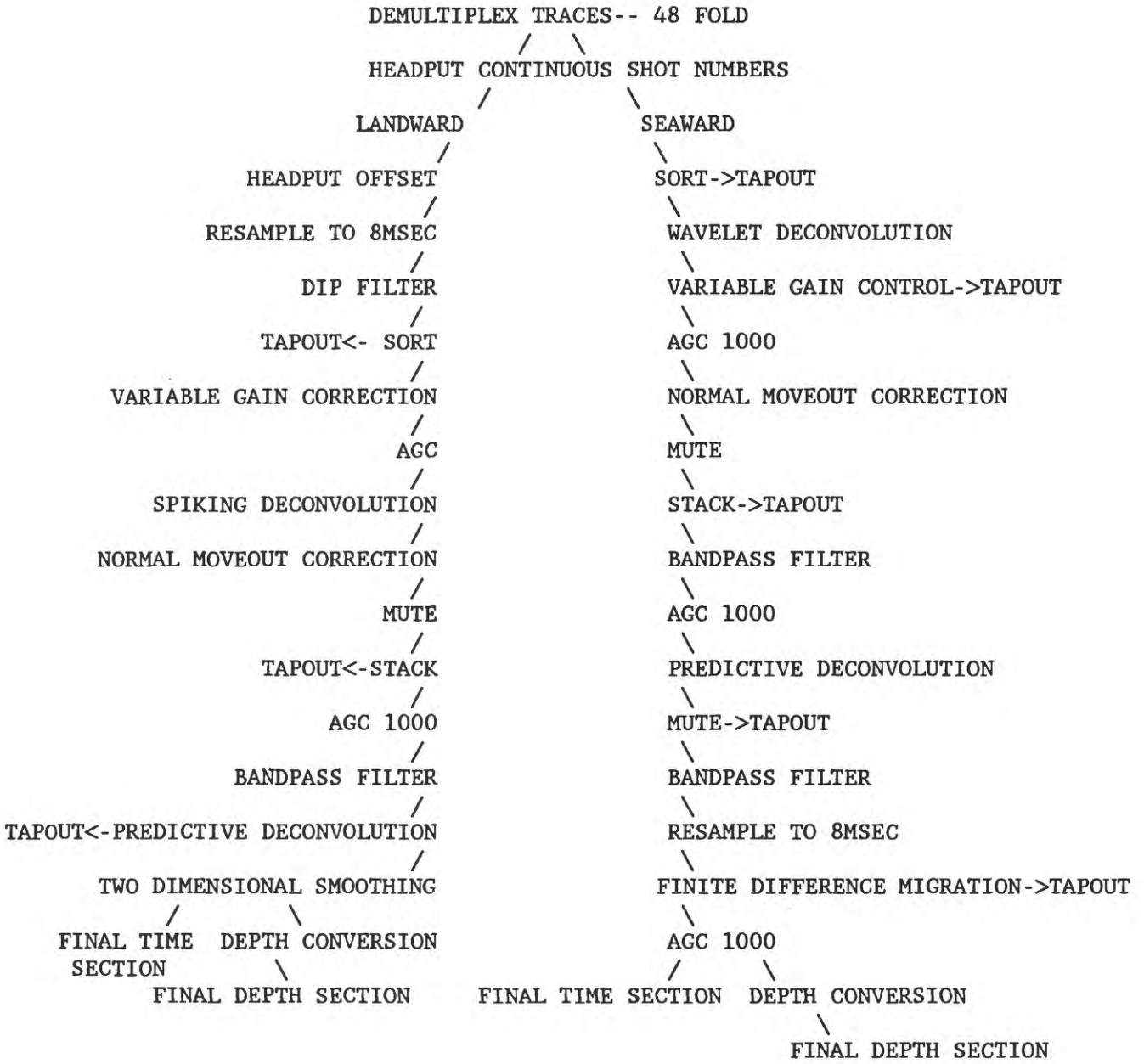

The last step was to depth convert the section (Figure 8). Velocities were obtained from a data set that is based on functions that are smoothed basin-wide and which have been checked for correlation between lines (K.D. Klitgord, unpublished data, 1987).

SEAWARD SECTION

The seaward section of the line covers a Jurassic-Cretaceous reef complex that is undergoing a detailed stratigraphic interpretation. Details of the structure and surrounding events, the presence or absence of internal reflectors within the carbonate structure, and continuity of reflectors are of great interest to researchers and thus, resolution and polarity of the seismic events were very important considerations in the reprocessing.

Seismic resolution depends not only on the frequency bandwidth of the source wavelet but also on the phase of the wavelet. Within the same frequency content, the zero-phase wavelet provides the optimum resolution power (Schoenberger, 1974). Spiking deconvolution is the most conventional and robust technique used to increase resolution, and it works well when the source signature is minimum phase and the earth reflectivity is close to being white. However, the spiking deconvolution rarely corrects the phase of the wavelet to a desired zero-phase as a result of (1) the failure of the assumptions regarding the source signature and earth reflectivity series, and (2) the presence of random noise in the real data. Wavelet processing was necessary to clarify the polarity of reflections as well as to increase the seismic resolution.

No source signature measurements were available for these data, so the wavelet was estimated from a CDP gather by a variable norm deconvolution method (Gray, 1978). The source signature was extracted from the 100 ms window after onset of the water-bottom reflections at CDP 2700. Based on the extracted wavelet, an inverse filter was designed using a zero-phase band pass filter (4/8-50/62 Hz) as the desired wavelet. This inverse filter was applied to the seaward part of line 6 (CDP range 2300-3215) after a routine sort by CDP of the demultiplexed traces. The assumption is made that the source signature does not change noticeably along this part of the line.

After the data were passed through the wavelet deconvolution filter, a variable gain compensation function and an AGC over 1000 ms gates were applied, followed by a NMO correction. Direct arrivals and refracted waves were muted before the data were stacked (Figures 3B,C). Stacking velocities were supplied every 50 CDP's (2.5 km) except in the area of the reef complex where velocity functions were picked every 12 to 25 CDP's (0.6 to 1.25 km). This was done to minimize any possible smearing of features.

Post-stack processing consisted of three main phases: (1) a second deconvolution filter and mute, (2) migration, and (3) depth conversion. The deconvolution was preceded by a depth and shot point variant bandpass filter and an AGC application over a 1000 ms window. A gap (predictive) deconvolution filter was applied where the gap was measured by the number of autocorrelation second zero crossings, and 0.1% white noise was added. This filter design varied with shot point. Another mute was applied as well, to allow for better

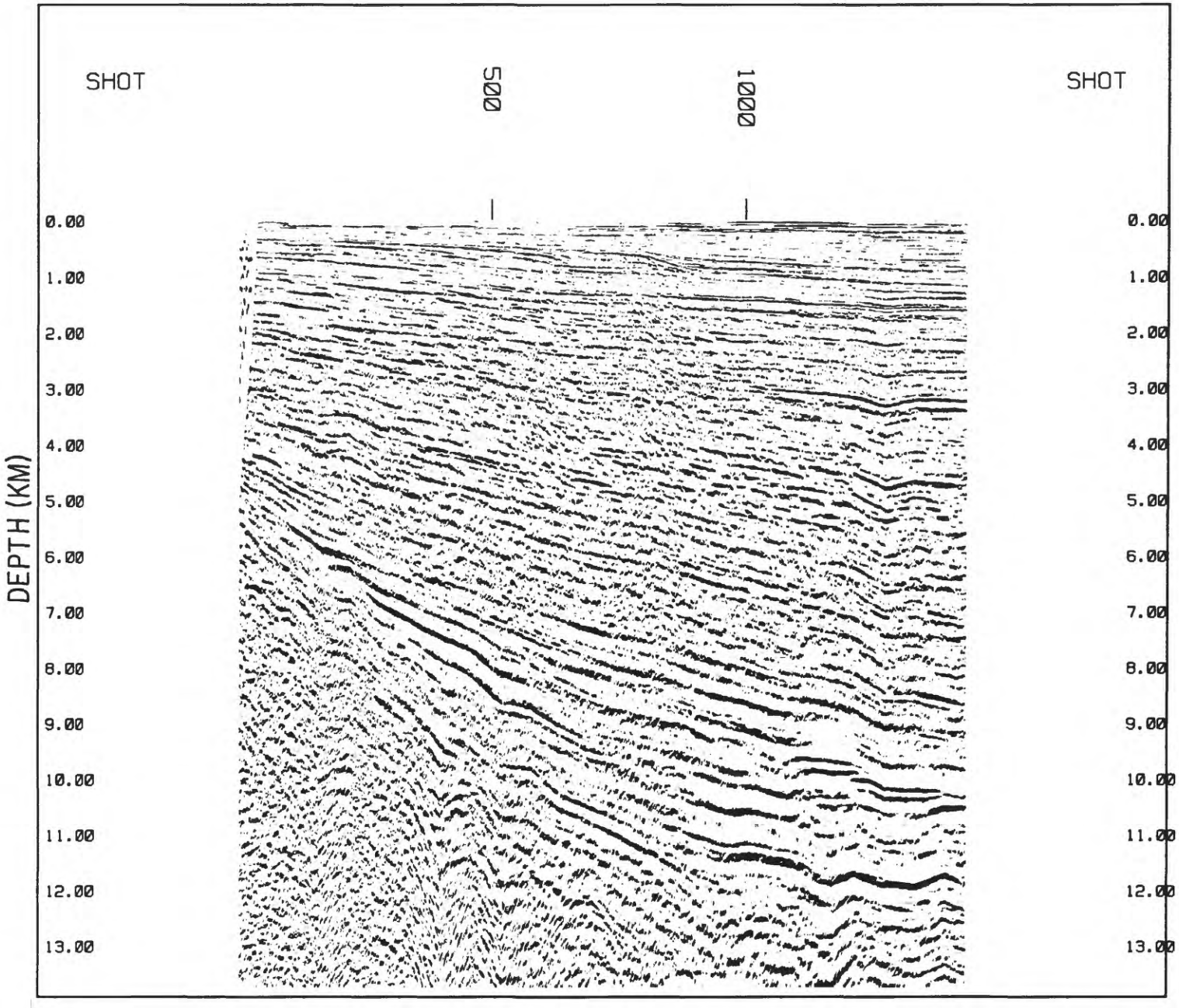

FIGURE 8: Depth converted landward section of line 6 with two-dimensional smoothing applied for display.

definition of the water bottom. The reprocessed section can be compared with the GSI section at this point (Figure 9A,B).

The migration was preceeded by bandpass filtering over the entire 0-11 s range with 4/8 to 42/52 Hz passed. The data were resampled to 8 ms, from the original 4 ms to decrease processing time. Different, simplified velocity functions are needed for the migration for two reasons: currently available finite difference migration algorithms cannot properly handle abrupt lateral velocity changes, and a migration algorithm uses true interval velocities, not stacking velocities or interval velocities. The latter are usually higher in value than true interval velocities, primarily due to structure and offset effects in the stacking velocities. Migration velocities used for reprocessing were derived on the basis of constant-velocity migration tests in the frequency-wavenumber (F-K) domain, which yield appropriate velocity ranges. The finite difference migration, we used is a time migration which images reflectors (e.g., collapses diffractions) to their 'true' subsurface position or reflecting interface. This improves lateral resolution and corrects for the distorted position of reflectors (Figure 10A). A depth section was generated using velocities from the same suite of smoothed functions described earlier (Figure 11).

A comparison was made to determine the effect of the spacing of velocity picks on the sharpness and continuity of features in the approximately 18-km-wide reef complex. A section that spans the reef complex was selected and the data were processed using the same velocity functions, only at an interval of 50 CDP's (2.5 km) to approximate the 3-km spacing of the GSI processed section (Figure 10B). There is little or no change in the section processed with less frequent velocity picks. Although the changes in the data due to differences in processing sequences make it important to repick velocities when reprocessing, we found that intervals closer than 50 CDP's are not necessary.

RESULTS

Reprocessing of the landward end of the line greatly enhanced the resolution and continuity of reflectors. This is a function of first removing the coherent noise by F-K filtering in the shot domain and then applying the two deconvolution operators. The benefits of 48-fold vs. 36-fold coverage are not great, providing only slight improvement in the signal-to-noise ratio. Actually, any processing of collected data with this nonlinear geometry would be simplified by using 36-fold shots because dip filtering would be greatly streamlined with the linear system and the processing time would decrease by about 10 percent.

The data have been greatly improved by reprocessing. The section of Line 6 covering the Jurassic reef complex shows an improvement in the definition of features, especially the pinnacled reef front. Amplitude recovery and proper migration have allowed more detailed interpretation of the structure. The wavelet deconvolution operator improved resolution of internal reflectors, especially those relative to the higher impedance contrast carbonate layers. The pinnacle reef at the seaward end of the complex is now definable as such, where it was obscured by diffractions in the original section (Figure 9A,B). The depth conversion has allowed more in-depth reanalysis of the data especially

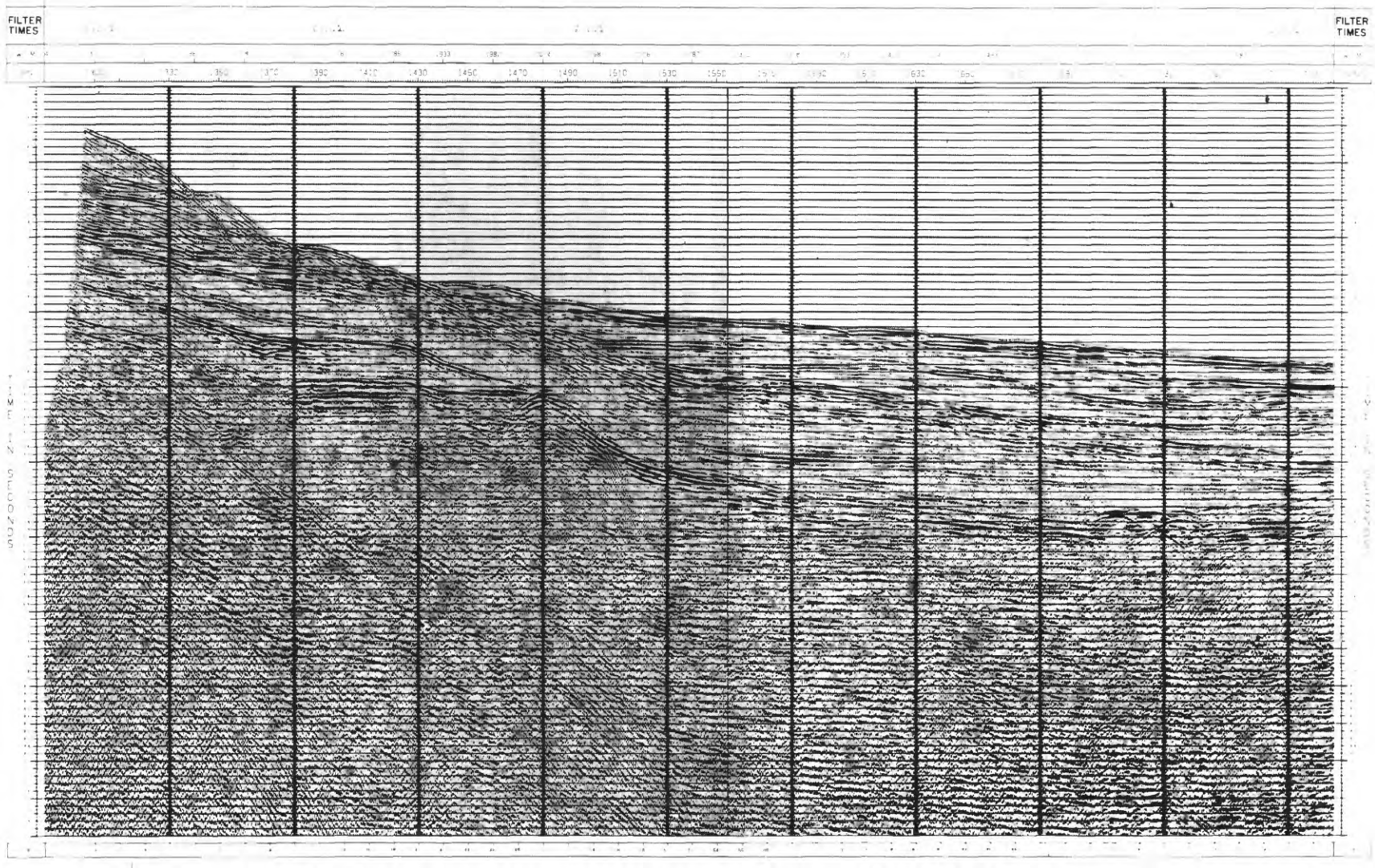

FIGURE 9: Comparison of time sections in the shelf complex area.
A: GSI section.

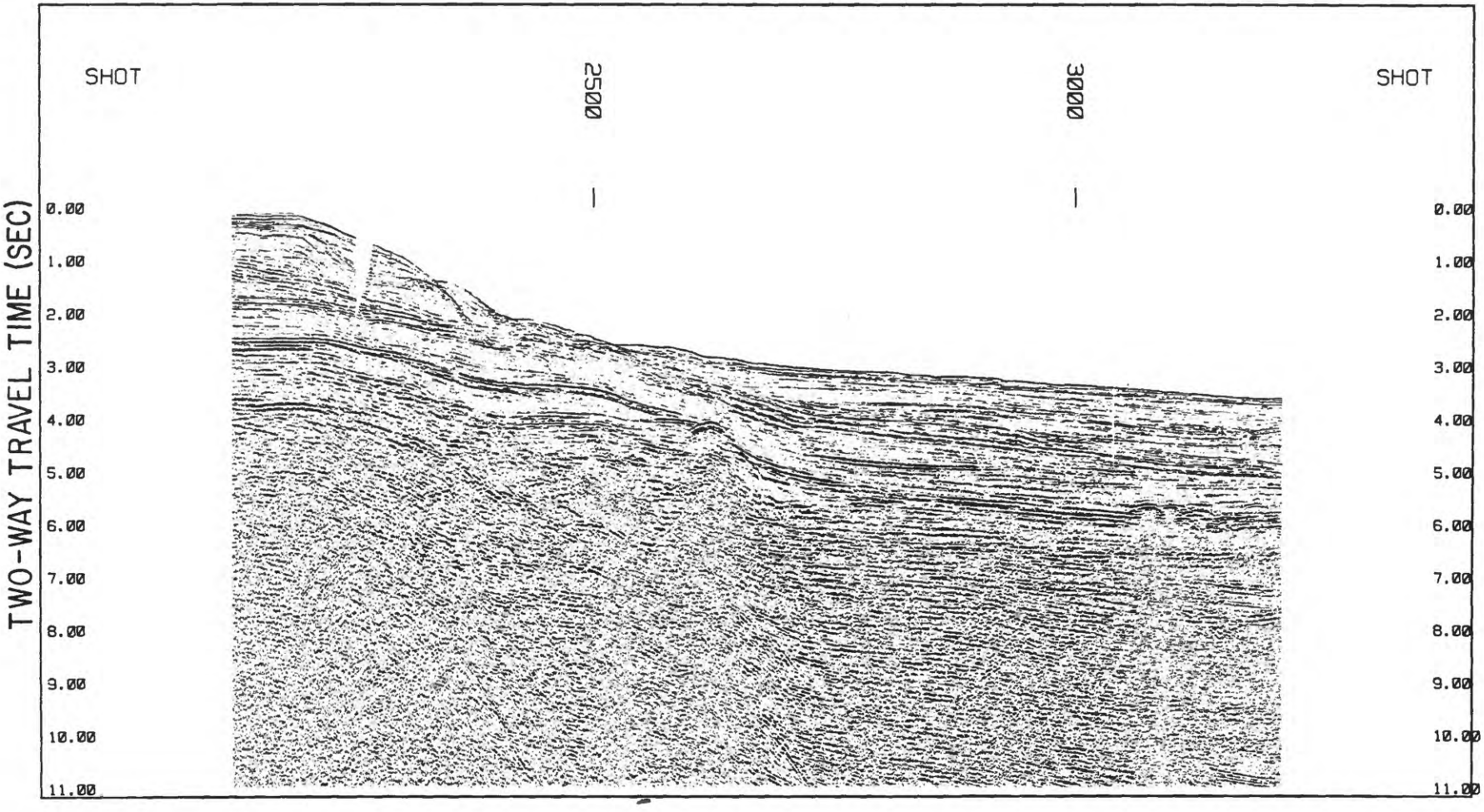

FIGURE 9B: Reprocessed time section -- no migration.

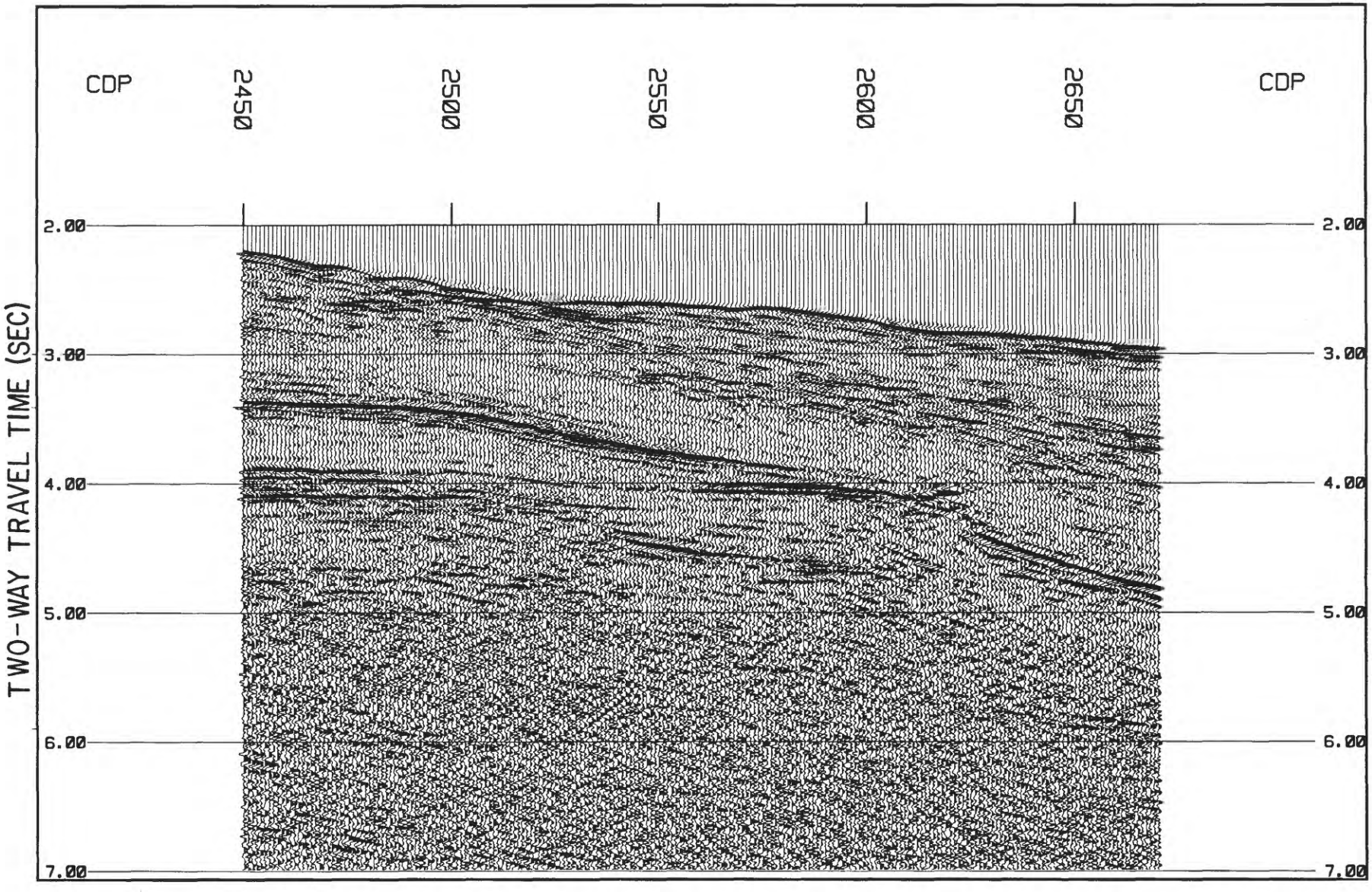

FIGURE 10: Velocity comparison in area of reef complex.
A: Migrated section processed with velocity picks every 12-25 CDP's (0.6 to 1.25 km).

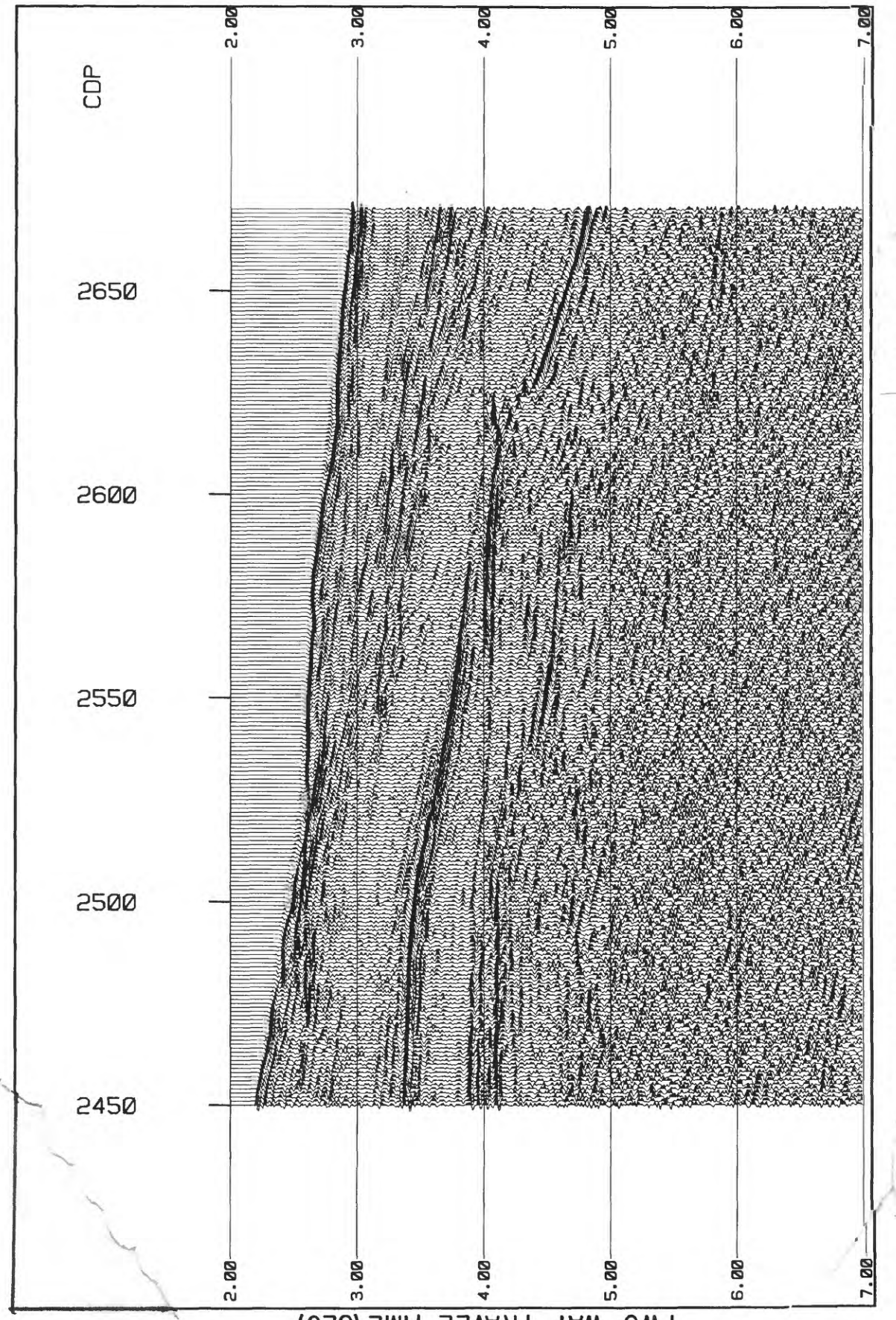

FIGURE B: Migrated section processed with velocity picks every 50 CDP's (2.5 km).

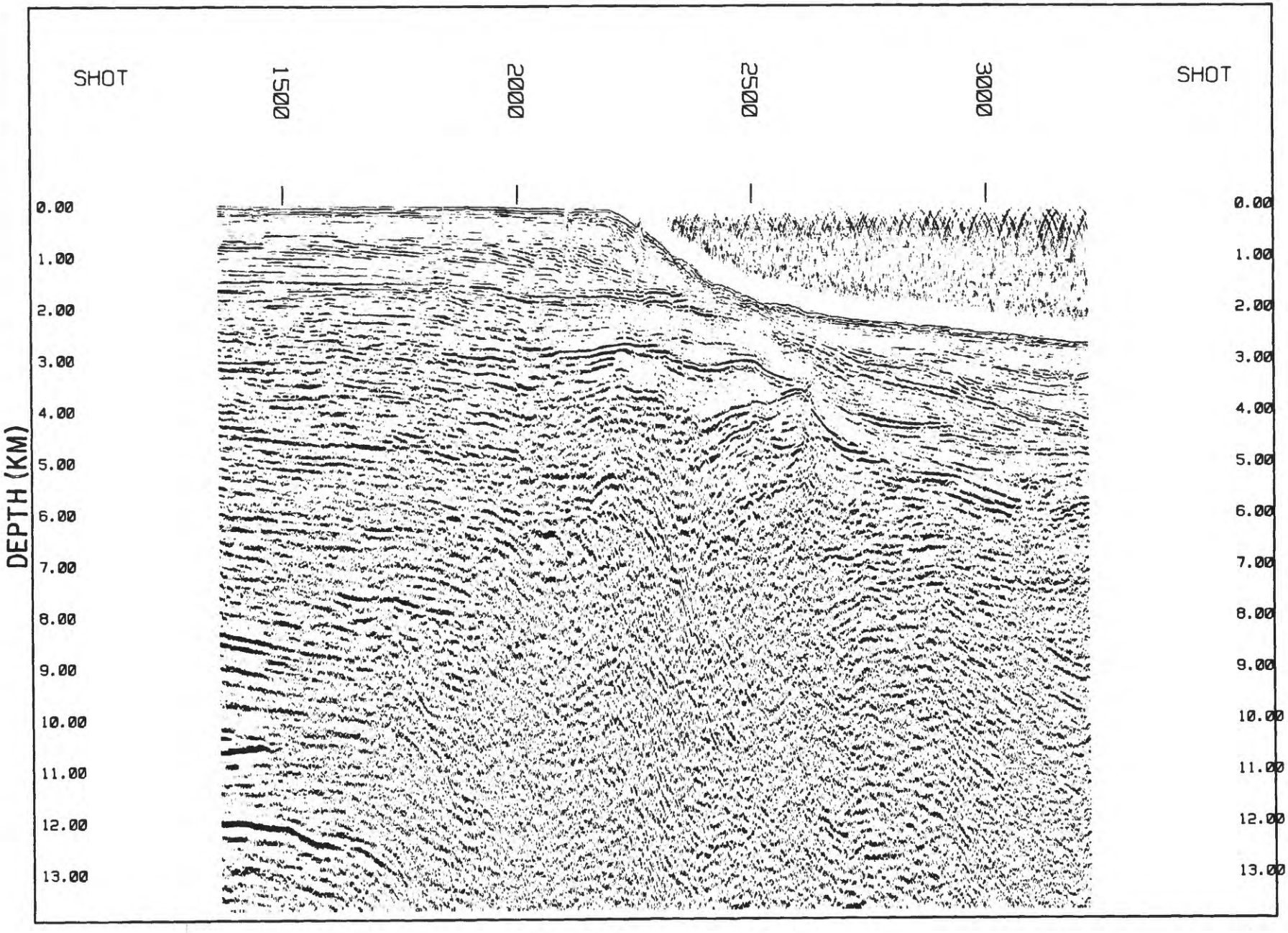

FIGURE 11: Depth converted migrated section -- seaward end of Line 6 with two-dimensional smoothing applied for display.

those that pertain to questions of basin and reef-complex evolution. The balance of the data are currently being reprocessed and are expected to yield similar enhancement and clarification.

ACKNOWLEDGEMENTS

We thank D. Hutchinson and N. Zihlman for assistance with the processing. Technical reviews by D.R. Hutchinson and J.S. Schlee were helpful. K.D. Klitgord provided smoothed, correlated velocities used in the depth conversion. Patty Forrestel, Jeffrey Zwinakis, and Dann Blackwood drafted and photographed the figures. All processing routines used are part of the Digicon DISCO software package or are routines developed by Myung Lee in house.

REFERENCES

Gray, W.C., 1978, Variable norm deconvolution: Palo Alto, Calif., Stanford Univ., Ph.D. thesis.

Larner, K., Chambers, R., Yang, M., Lynn, W., and Wai, W., 1983, Coherent noise in marine seismic data: Geophysics, v. 48, p. 854-886.

Lee, M.W., Agena, W.F. and Hutchinson, D.R., 1988, Processing of the GLIMPCE multichannel Seismic Data: U.S. Geological Survey Open-File Report 88-225.

Schoenberger, M., 1974, Resolution comparision of minimum-phase and zero-phase signals: Geophysics, v. 39, p. 826-833.